

# Distillation Kinetics of Solid Mixtures of Hydrogen Peroxide and Water and the Isolation of Pure Hydrogen Peroxide in Ultrahigh Vacuum

M. J. Loeffler,\* B. D. Teolis,<sup>†</sup> and R. A. Baragiola<sup>‡</sup>

Laboratory for Atomic and Surface Physics, Thornton Hall, University of Virginia,  
Charlottesville, Virginia 22904-4238

Received: January 15, 2006; In Final Form: February 8, 2006

We present results of the growth of thin films of crystalline  $\text{H}_2\text{O}_2$  and  $\text{H}_2\text{O}_2 \cdot 2\text{H}_2\text{O}$  (dihydrate) in ultrahigh vacuum by distilling an aqueous solution of hydrogen peroxide. We traced the process using infrared reflectance spectroscopy, mass loss on a quartz crystal microbalance, and in a few cases ultraviolet–visible reflectance. We find that the different crystalline phases—water, dihydrate, and hydrogen peroxide—have very different sublimation rates, making distillation efficient to isolate the less volatile component, crystalline  $\text{H}_2\text{O}_2$ .

## Introduction

Solid hydrogen peroxide is an interesting material for being one of the simplest molecular solids, and for its role in cold astrophysical environments and in the upper atmosphere of the Earth.<sup>1</sup> The recent discovery of  $\text{H}_2\text{O}_2$  on the surface of one of Jupiter's icy moons, Europa,<sup>2</sup> has renewed the interest in this substance and prompted studies inquiring how  $\text{H}_2\text{O}_2$  can form in that environment,<sup>3–6</sup> and whether it occurs in pure form or in a solid solution with water.<sup>7,8</sup>

The properties of solid  $\text{H}_2\text{O}_2\text{--H}_2\text{O}$  solutions are barely known. Early X-ray diffraction measurements<sup>9</sup> showed that an intermediate compound phase exists in crystalline mixtures, the dihydrate  $\text{H}_2\text{O}_2 \cdot 2\text{H}_2\text{O}$ . This compound was also identified in the determination of the equilibrium phase diagram of water–hydrogen peroxide,<sup>10</sup> indicating that when solutions approach equilibrium, there is a competition between the formation of three phases: water ice,  $\text{H}_2\text{O}_2$ , and the dihydrate. This dihydrate phase was subsequently identified using infrared spectroscopy.<sup>11</sup> The temperatures at which the dihydrate formed in those experiments (140–200 K) were similar to those on the warmer icy satellites of Jupiter. This prompted us to study the different phases in a vacuum to establish the conditions under which the dihydrate may form in outer space and also to advance understanding of the underlying physicochemical processes.

The scarcity of studies on either pure solid  $\text{H}_2\text{O}_2$  or aqueous solutions in a vacuum environment is due partly to the difficulty in containing this reactive molecule and partly because high concentrations of  $\text{H}_2\text{O}_2$  are no longer commercially available. Recently, there has been a report of success in growing  $\text{H}_2\text{O}_2$  in a vacuum by vapor deposition of gaseous  $\text{H}_2\text{O}_2$  from urea hydrogen peroxide in a vacuum.<sup>12</sup> We do not follow this method here since we have found that it is inefficient for producing pure solid-phase  $\text{H}_2\text{O}_2$  by vapor deposition. Instead, we explored the possibility of obtaining pure  $\text{H}_2\text{O}_2$  and its compound by distillation of an aqueous solution in a vacuum *after* it is deposited on the substrate, taking advantage of the higher sublimation rate of water than of hydrogen peroxide. The

potential of this technique was demonstrated in a previous study of evaporation of a water ice film containing  $\text{H}_2\text{O}_2$  produced by ion irradiation.<sup>3</sup> Here we present measurements showing the isolation of crystalline  $\text{H}_2\text{O}_2$  deposits by distillation in ultrahigh vacuum, where we monitor the composition with infrared spectroscopy and the mass loss due to sublimation with a microbalance.

## Experimental Setup

All experiments were performed on a radiation-shielded cryostat inside a stainless steel vacuum chamber;<sup>3</sup> the base pressure was  $(1\text{--}4) \times 10^{-9}$  Torr and 1–2 orders of magnitude lower inside the shield.  $\text{H}_2\text{O}_2\text{--H}_2\text{O}$  ice films were grown by vapor deposition using a stainless steel manifold that was passivated by boiling an aqueous solution of 30 wt %  $\text{H}_2\text{O}_2$  (Alfa Aesar) under oil-free vacuum. This procedure cleansed hydrocarbons on the internal walls of the manifold, thereby reducing production of volatile impurities, such as CO,  $\text{CO}_2$ , and  $\text{O}_2$ , generated by reactions of the  $\text{H}_2\text{O}_2$  with the hydrocarbons. The temperature of the glass ampule containing the solution was held at  $\sim 100^\circ\text{C}$  to increase the pressure of  $\text{H}_2\text{O}_2$  in the manifold. The films were deposited on the gold mirror electrode of a 6 MHz quartz-crystal microbalance (QCM), which measures the areal mass  $Q$  (mass/unit area).<sup>13</sup> The deposition temperatures were in the range of 150–173 K, where we determined that the sticking of impurities was undetectable. After growing films in the range of 6–130  $\mu\text{g}/\text{cm}^2$ , we held them at a constant temperature and monitored the mass loss due to sublimation of water and hydrogen peroxide. Since the latter has a lower sublimation rate than water, the concentration of  $\text{H}_2\text{O}_2$  in the film increases with time; i.e., we distill the film.

The specular infrared reflectance of the films on the gold mirror was measured at an incident angle of  $35^\circ$  with a Thermo-Nicolet Nexus 670 Fourier transform infrared spectrometer at 2  $\text{cm}^{-1}$  resolution, while the specular UV–visible reflectance was measured at an incident angle of  $22.5^\circ$  with an Ocean Optics CCD spectrometer. In both cases, we normalized the spectra by dividing them by the spectrum of the bare gold mirror substrate. In the following we show the normalized spectra in reflectance units  $R$  or the optical depth, given by  $-\ln R$  (Figure 1). To elucidate compositional changes in the films as a result of desorption, we used a differential method: we subtracted

\* To whom correspondence should be addressed. Phone: (434) 924-1059. Fax: (434) 924-1059. E-mail: mjl8r@virginia.edu.

<sup>†</sup> E-mail: bdt4z@virginia.edu.

<sup>‡</sup> E-mail: raul@virginia.edu.

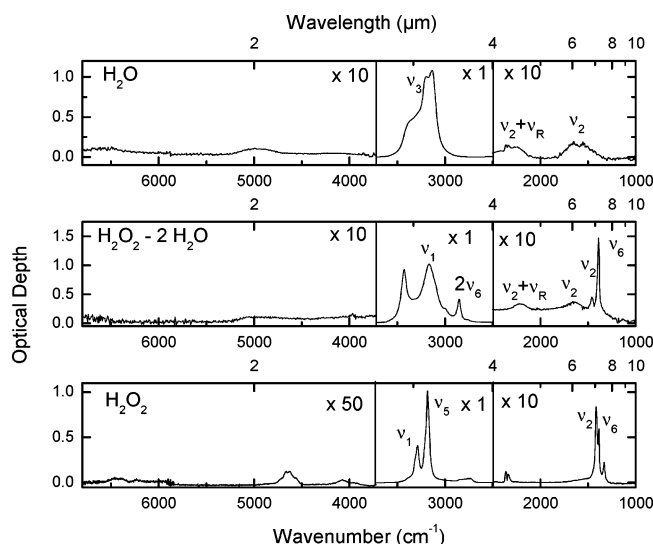


**Figure 1.** Top: Infrared spectrum of a 30  $\mu\text{g}/\text{cm}^2$  film of crystalline water ice taken at 155 K. Middle: Infrared spectrum of a 15  $\mu\text{g}/\text{cm}^2$  film of the compound  $\text{H}_2\text{O}_2 \cdot 2\text{H}_2\text{O}$  distilled at 158 K (see text). Bottom: Infrared spectrum of a 36  $\mu\text{g}/\text{cm}^2$   $\text{H}_2\text{O}_2$  distilled at 166 K (the peaks in the 2300  $\text{cm}^{-1}$  region in this graph are due to residual gas-phase  $\text{CO}_2$ ). The labels correspond to transitions that have been identified by Giguere and Harvey.<sup>11</sup>

**TABLE 1:  $\text{H}_2\text{O}_2 \cdot 2\text{H}_2\text{O}$  Dihydrate Absorption Bands ( $\text{cm}^{-1}$ )<sup>a</sup>**

peak position	assignment	peak position	assignment
1391.4(8), m	$\nu_6$	2852(1), s	$2\nu_6$
1459.6(10), w	$\nu_2$	2997(2), vw	
1648(8) broad, w	$\nu_2$ ( $\text{H}_2\text{O}$ )	3165(1), vs	$\nu_1$
2212(6) broad, w	$\nu_2 + \nu_R$ ( $\text{H}_2\text{O}$ )	3427(1), vs	
2753(2), vw		5053(20) broad vw	

<sup>a</sup> Assignments based on Giguere and Harvey.<sup>11</sup> Sh, shoulder. Qualitative absorption strengths are indicated by the following: s, strong; m, medium; w, weak; vw, very weak. The numbers in parentheses are uncertainties in the last significant figure.

successive optical depth spectra and attributed the difference to the material that desorbed between the measurements.

## Results and Discussion

**Crystalline Dihydrate Compound and Crystalline  $\text{H}_2\text{O}_2$ .** The equilibrium phase diagram of the  $\text{H}_2\text{O}_2$ – $\text{H}_2\text{O}$  system<sup>10</sup> for  $\text{H}_2\text{O}_2$  concentrations below that of the dihydrate shows that the only phases are solid water and dihydrate; no pure hydrogen peroxide precipitates are expected.<sup>10</sup> Conversely, at  $\text{H}_2\text{O}_2$  concentrations higher than that of the dihydrate (48.6 wt %), the equilibrium phases are the dihydrate and pure hydrogen peroxide. Equilibrium phases are not expected when solutions are condensed below about 120 K, where molecular diffusion is extremely slow in laboratory time scales. However, our experiments were conducted above 150 K, where the equilibrium phases form almost instantaneously. Therefore, the infrared spectrum of the solid solutions have the signatures of water, the dihydrate compound  $\text{H}_2\text{O}_2 \cdot 2\text{H}_2\text{O}$ , and pure  $\text{H}_2\text{O}_2$  (Figure 1 and Tables 1 and 2), depending on the  $\text{H}_2\text{O}_2$  concentration. It is important to note that since the experiments are done in a vacuum, the continuous evaporation implies that we are moving gradually in the phase diagram toward regions of higher  $\text{H}_2\text{O}_2$  concentration.

We performed distillation of  $\text{H}_2\text{O}_2$ – $\text{H}_2\text{O}$  mixtures at two temperatures: 154.4 and 166 K. After the film was deposited at 154.4 K, the optical depth spectra (Figures 2 and 3, compared to Figure 1) show that both water and hydrogen peroxide leave the film, with water being lost preferentially. In addition, we

**TABLE 2: Crystalline  $\text{H}_2\text{O}_2$  Absorption Bands ( $\text{cm}^{-1}$ )<sup>a</sup>**

peak position	assignment	peak position	assignment
1332.5(10), m	$2\nu_4$	3182.2(4), vs	$\nu_5$
1388.4(10), s	$\nu_6$	3287.1(6), vs	$\nu_1$
1416.5(10), s	$\nu_2$	3316(4), sh	
2264(3), vw		3392(3)	
2337.5(5), m		3957(10), sh	
2362.0(5), m		4075(7) broad, vw	
2395(1), vw		4566(10), sh	
2460(5) broad, vw		4628(3), w	
2730(3), sh		4664(2), w	
2754 (2), m		4725 (10), (sh)	
2805(3), m		6220 plateau, vw	
2843(3), m		6425(20) broad, vw	

<sup>a</sup> Assignments are from Giguere and Harvey.<sup>11</sup> Sh, shoulder. Qualitative absorption strengths are indicated by the following: s, strong; m, medium; w, weak; vw, very weak. The numbers in parentheses are uncertainties in the last significant figure.

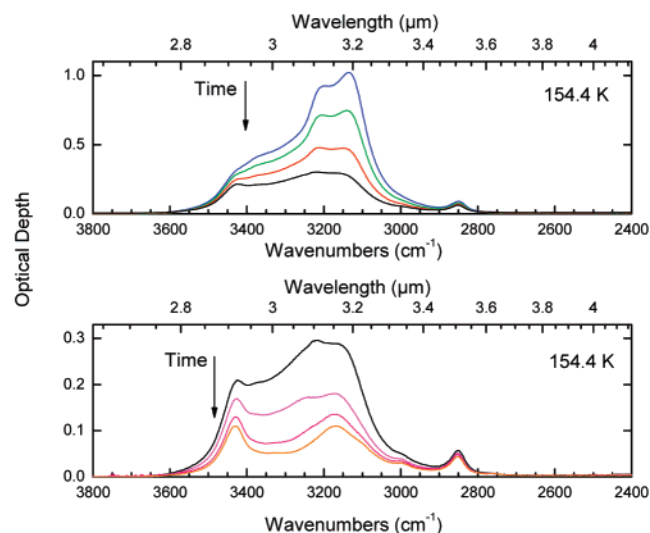


**Figure 2.** Subset of the infrared spectra taken during isothermal distillation of a 30.6  $\mu\text{g}/\text{cm}^2$  mixture of water ice and hydrogen peroxide at 154.4 K. During the experiment, there is mass loss due to sublimation. The residual areal masses of the films as time progresses are as follows: (top panel) 30.6, 28.1, 22.9, and 18.7  $\mu\text{g}/\text{cm}^2$ ; (bottom panel) 18.7, 13.9, 9.0, and 7.36  $\mu\text{g}/\text{cm}^2$ . The film with the highest mass (top curve) is a mixture of crystalline water and crystalline  $\text{H}_2\text{O}_2 \cdot 2\text{H}_2\text{O}$ , while the film with the lowest mass (bottom curve) is crystalline  $\text{H}_2\text{O}_2 \cdot 2\text{H}_2\text{O}$ .

obtained mass loss rates due to sublimation by taking the time derivative of the areal mass given by the QCM. Figure 4 shows that the sublimation rate decreases with time, while significant changes occur in the differential infrared signature of the desorbing species (Figure 5). By the time there is 7.36  $\mu\text{g}/\text{cm}^2$  remaining on the substrate (Figure 2), pure water (i.e. not bonded to the dihydrate) has nearly disappeared by desorption. The infrared spectrum corresponds to that of the pure compound since there is no evidence for the broad band at 3.6  $\mu\text{m}$  characteristic of crystalline  $\text{H}_2\text{O}_2$ . We note that the transition from water plus dihydrate to only dihydrate seen in the infrared spectrum between 9.6 and 7.3  $\mu\text{g}/\text{cm}^2$  (Figure 2) is accompanied by a change in the sublimation rate (at  $\sim 6700$  to  $8100$  s in Figure 4). At the same time, the bending bands of  $\text{H}_2\text{O}_2$  in the infrared spectra change only slightly due to the loss of water (Figure 3). Incidentally, the fact that the asymmetric bend ( $\nu_6$ ) absorption is much stronger than the symmetric ( $\nu_2$ ) bend supports the view that the 3.5  $\mu\text{m}$  absorption feature is an overtone of  $\nu_6$ <sup>11</sup> rather than of  $\nu_2$ . At longer times the concentration of  $\text{H}_2\text{O}_2$  rose above that of the dihydrate and the

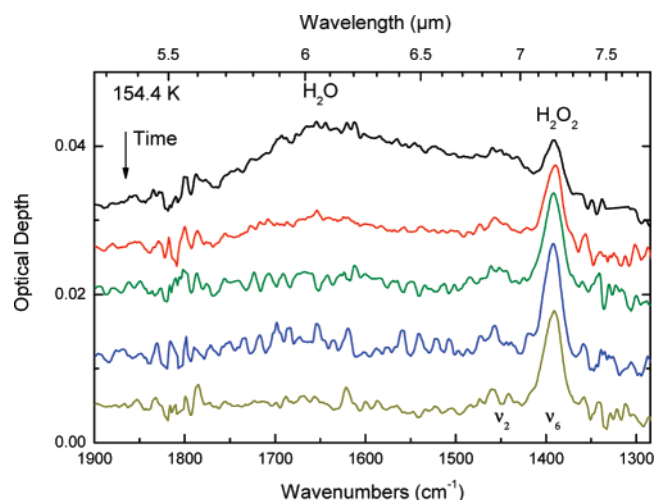


**Figure 3.** Infrared spectra of the bending region of a water-hydrogen peroxide mixture during isothermal distillation at 154.4 K for the same film as shown in Figure 2. The residual areal masses of the films as time progresses are as follows: 30.6, 18.7, 13.9, 9.0, and 7.36  $\mu\text{g}/\text{cm}^2$ . The film with the highest mass (top curve) is a mixture of crystalline water and crystalline  $\text{H}_2\text{O}_2 \cdot 2\text{H}_2\text{O}$ , while the film with the lowest mass (bottom curve) is crystalline  $\text{H}_2\text{O}_2 \cdot 2\text{H}_2\text{O}$ . The spectra have been displaced vertically for clarity.

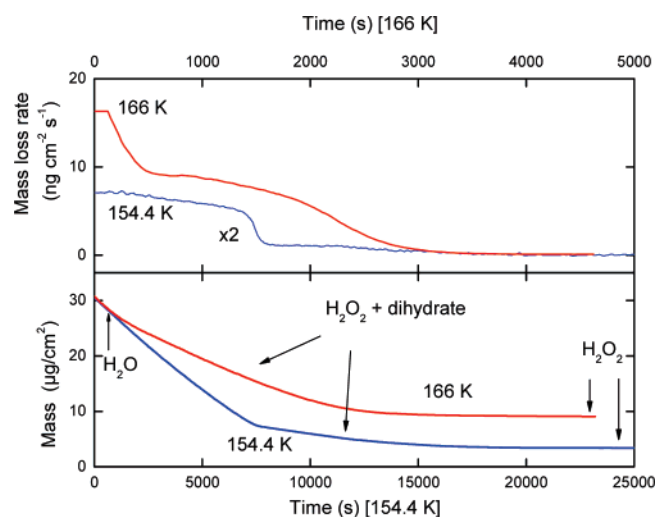


**Figure 4.** Mass change (bottom) and mass loss rate (top) of the films during distillation and sublimation. Note that the time scale is reduced by a factor of 5 for plotting the 166 K experiments. The infrared spectra taken during the 154.4 and 166 K experiments appear in Figures 2, 3 and Figures 6, 7, respectively.

infrared spectra showed that the film eventually became pure  $\text{H}_2\text{O}_2$ ,<sup>14</sup> with negligible sublimation rate (Figure 4, top).

Now we analyze the case of films deposited at a higher temperature: 166 K. In this case, the as-deposited film is similar in thickness to the one grown at 154.4 K but it has a higher  $\text{H}_2\text{O}_2$  concentration (and amount) because of a decreased sticking coefficient of water.<sup>15</sup> At 166 K, the distillation proceeded as at 154.4 K but with a reduced time scale due to higher sublimation rates. We note that the sublimation rate during the experiments dropped by nearly 2 orders of magnitude when going from the sublimation of water to that of hydrogen peroxide (Figure 4, top). In Figures 6 and 7, we show the evolution of optical depth spectra (beginning at  $15.3 \mu\text{g}/\text{cm}^2$  at  $\sim 1500$  s in Figure 4) after crystalline water has already desorbed and only the dihydrate and pure  $\text{H}_2\text{O}_2$  remain on the substrate. Late in the distillation, the stretching vibrations  $\nu_1$  and  $\nu_5$  (Figure 6), bending vibrations  $\nu_2$  and  $\nu_6$  (Figure 7), and bending overtone

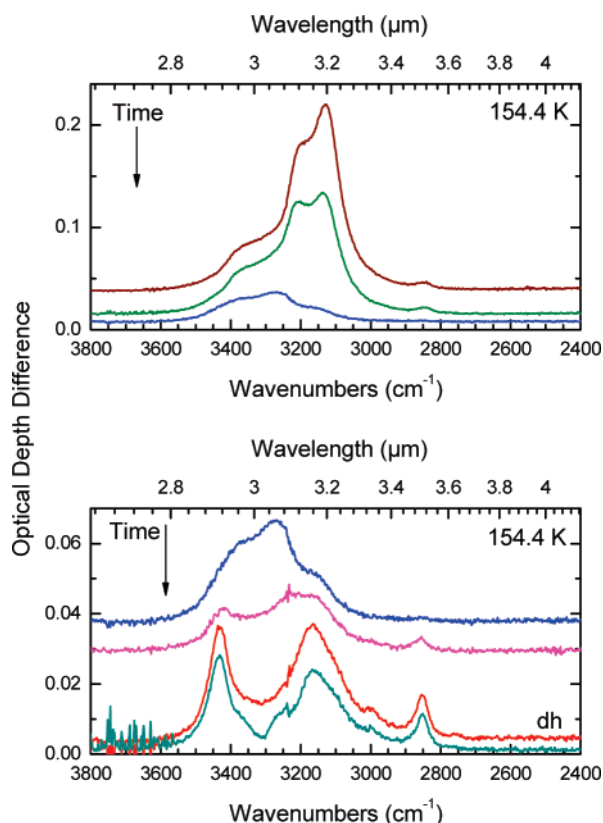


**Figure 5.** Subset of the infrared spectra taken during isothermal distillation of a  $30.6 \mu\text{g}/\text{cm}^2$  film at 154.4 K viewed from a different perspective. Successive spectra were subtracted; thus, the spectral differences correspond to the material that has sublimed. The areal masses of the desorbed material as time progresses are as follows: (top panel) 2.06, 1.95, and  $1.65 \mu\text{g}/\text{cm}^2$ ; (bottom panel) 1.65, 1.38, 1.14, and  $1.02 \mu\text{g}/\text{cm}^2$ . The corresponding residual areal masses of the film at the end of each step are as follows: (top panel) 26.9, 20.8, and  $9.82 \mu\text{g}/\text{cm}^2$ ; (bottom panel) 9.82, 8.09, 6.05, and  $5.08 \mu\text{g}/\text{cm}^2$ . We note that the spectrum labeled dh matches the shape of the dihydrate band. The spectra have been displaced vertically for clarity.

regions (Figure 8), characteristic of pure  $\text{H}_2\text{O}_2$ ,<sup>11,14</sup> are visible in the infrared spectra.

The crystalline  $\text{H}_2\text{O}_2$  films obtained at long times are very stable: after more than 12 h at 166 K, there were no observable changes in the infrared spectra besides a slight decrease of the absorption due to sublimation of the film. After distillation the purity of these films is  $\sim 98\%$  crystalline  $\text{H}_2\text{O}_2$ . This value is based on experiments where we added known amounts of water to  $\text{H}_2\text{O}_2$  while measuring the absorption band of water at  $\sim 1650 \text{ cm}^{-1}$ . The conclusion is also consistent with published spectra for films of approximately the same thickness.<sup>14</sup>

**Effect of Sublimation on Optical Reflectance.** We measured the UV–visible (300–700 nm) reflectance during film deposition at 100 and at 167 K. At 100 K we observed well-pronounced oscillations in reflectance between 300 and 500 nm caused by interference between reflections from the substrate and the film surfaces. In contrast, when the films were grown at 167 K, there was no indication of oscillations because the specular reflectance was attenuated by light scattering off the film. This effect was most prominent in the visible but also apparent in the infrared (Figure 9). This wavelength dependence (reddening) indicates Rayleigh scattering from small imperfections; their nature is not clear at present, but they may be boundaries between grains or precipitates, surface roughness, and microcracks, etc. These reflectance measurements were consistent with visual inspection of the film, which looked hazy



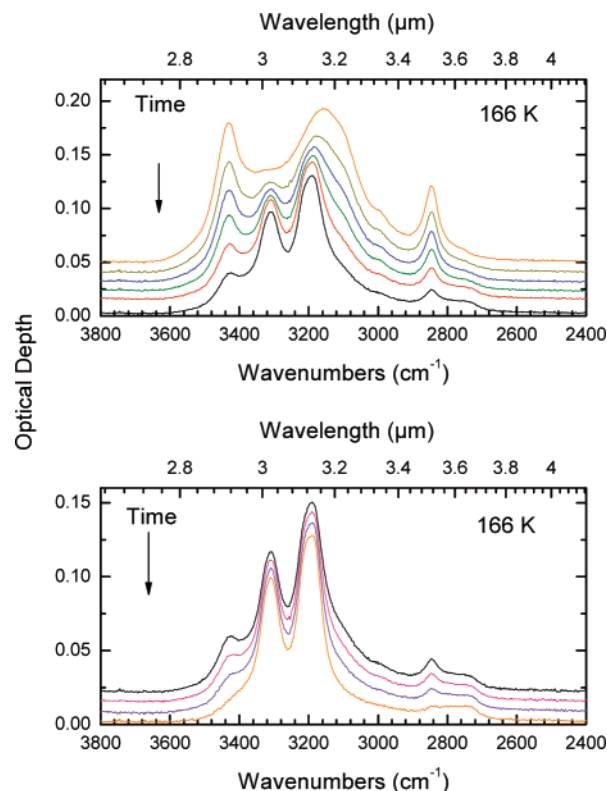


**Figure 6.** Subset of infrared spectra during isothermal distillation of an initially  $30.4 \mu\text{g}/\text{cm}^2$  water–hydrogen peroxide sample at 166 K, with concurrent mass loss due to sublimation. The residual areal mass of the films as time progresses are as follows: (top panel) 15.3, 13.9, 13.2, 12.3, 11.0, and  $10.8 \mu\text{g}/\text{cm}^2$ ; (bottom panel) 10.8, 10.2, 9.77, and  $9.17 \mu\text{g}/\text{cm}^2$ . The film with the highest mass (top curve) contains a crystalline mixture of  $\text{H}_2\text{O}_2$  and its dihydrate (see Figure 4), while that with the lowest mass (bottom curve) gives the spectrum of crystalline  $\text{H}_2\text{O}_2$ . The spectra have been displaced vertically for clarity.

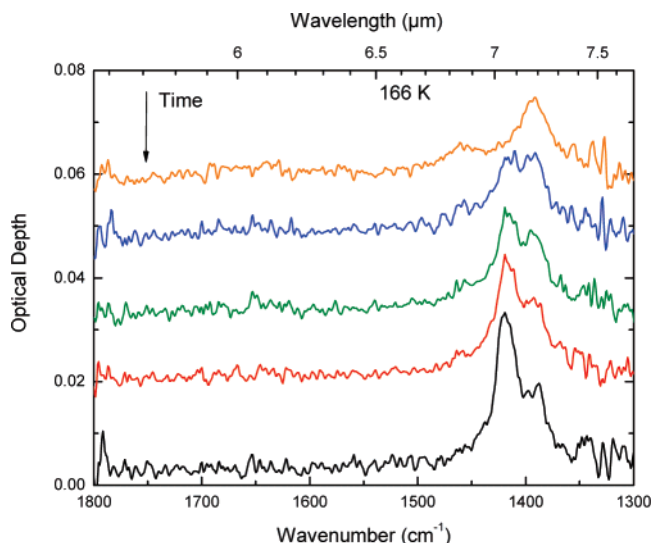


**Figure 7.** Infrared spectra of the  $\text{H}_2\text{O}_2$  bending region during crystallization at 166 K corresponding to Figure 6 for a residual mass of 15.3, 13.2, 12.3, 11.0, and  $9.17 \mu\text{g}/\text{cm}^2$ . The film with the highest mass (top curve) contains a crystalline mixture of  $\text{H}_2\text{O}_2$  and its dihydrate (see Figure 4), while that with the lowest mass (bottom curve) gives the spectrum of crystalline  $\text{H}_2\text{O}_2$ . The spectra were displaced vertically for clarity.

and nonuniform. Also in the specular direction the film appeared red to the eye.

After we stopped deposition at 167 K, we monitored the temporal changes in the sublimation rate and in the optical

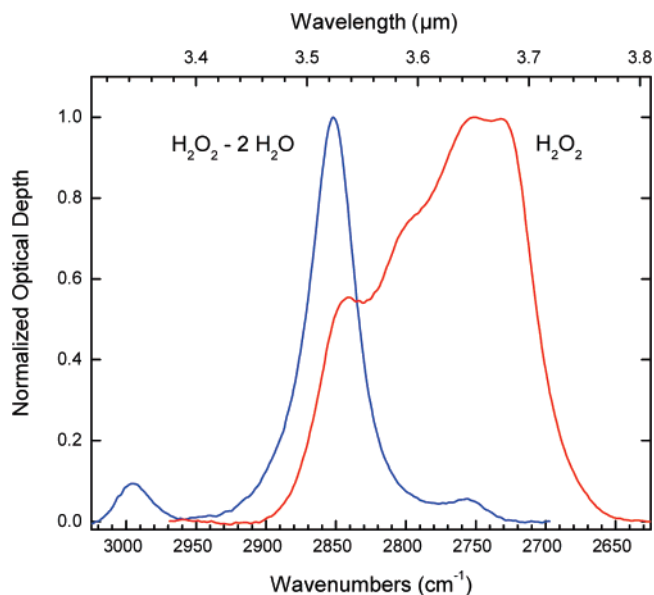


**Figure 8.** Comparison of the  $\sim 2800 \text{ cm}^{-1}$  infrared overtone bands of the dihydrate compound and crystalline  $\text{H}_2\text{O}_2$ . The bands have been normalized to better compare their shapes.

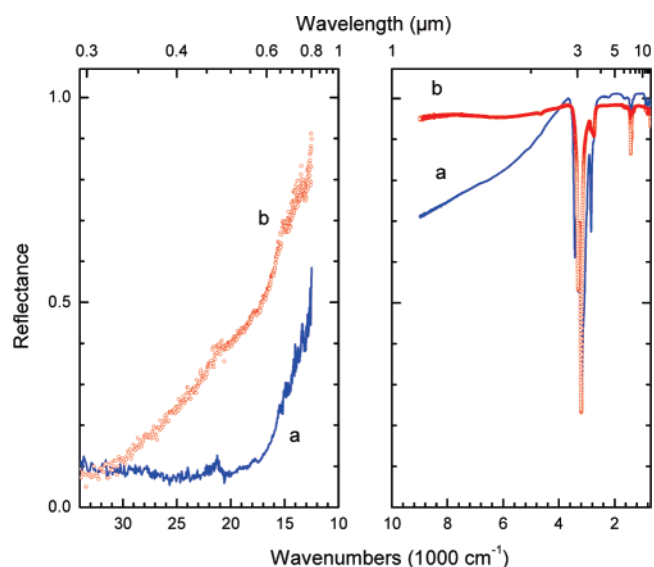


**Figure 9.** Ultraviolet–visible and infrared spectra of a water–hydrogen peroxide mixture after deposition at 167 K at two different times: (a) the end of deposition of  $45 \mu\text{g}/\text{cm}^2$  and (b) 9.5 h after deposition, when only  $25 \mu\text{g}/\text{cm}^2$  of pure  $\text{H}_2\text{O}_2$  remains. The weak structure at  $\sim 21\,000 \text{ cm}^{-1}$  is due to an incomplete cancellation of a sharp transition in the reflectance of the gold substrate.

reflectance of the sample. Sublimation proceeded similarly to that shown in Figure 4. After  $9\frac{1}{2}$  h, when the infrared spectrum showed the signature of only hydrogen peroxide, the specular reflectance in the visible and lower infrared wavelengths increased substantially (Figure 9), indicating a decrease in scattering. This effect may be due to homogenization of the film by loss of the dihydrate phase or by the growth of the  $\text{H}_2\text{O}_2$  precipitates. Visual inspection also supports the increase in homogeneity; we found that after the dihydrate sublimates the appearance of the reflected light to the eye changed from red to white and specular reflection became prominent, even though the film still appeared somewhat hazy in an off-specular position.

## Conclusions

Here we have demonstrated a method for the growth, in ultrahigh vacuum, of films of controlled composition of  $\text{H}_2\text{O}_2$  and  $\text{H}_2\text{O}_2 \cdot 2\text{H}_2\text{O}$  by distillation, avoiding the risk of decomposition or contamination by reactions with system walls. Above  $\sim 150$  K, different phases precipitate quickly, as expected from the equilibrium phase diagram. Sublimation results in the loss of material according to the volatility of the species: first water, then the dihydrate, and finally,  $\text{H}_2\text{O}_2$ , the least volatile. The use of the microbalance allows us to quantify the distillation process. At the higher temperatures tried in this study, 166–167 K, the decreased sticking of water molecules led to films with higher  $\text{H}_2\text{O}_2$  concentrations. Distillation resulted in crystalline  $\text{H}_2\text{O}_2$  with negligible amounts of impurities detectable by infrared spectroscopy. This method of preparation should be useful for further studies of pure hydrogen peroxide and could be extended to other reactive condensed gases, which are not easily handled in their pure form. Finally, our results show that the dihydrate compound may form at temperatures that exist in the mesosphere of the Earth and in warmer regions of the outer solar system.

**Acknowledgment.** This research was supported by NASA Planetary Atmospheres and NSF Astronomy programs. M.J.L. thanks the Virginia Space Grant Consortium for a scholarship.

## References and Notes

- (1) Jackson, A. V.; Hewitt, C. N. *Crit. Rev. Environ. Sci. Technol.* **1999**, *29*, 175.
- (2) Carlson, R. W.; Anderson, M. S.; Johnson, R. E.; Smythe, W. D.; Hendrix, A. R.; Barth, C. A.; Soderblom, L. A.; Hansen, G. B.; McCord, T. B.; Dalton, J. B.; Clark, R. N.; Shirley, J. H.; Ocampo, A. C.; Matson, D. L. *Science* **1999**, *283*, 2062.
- (3) Loeffler, M. J.; Raut, U.; Vidal, R. A.; Baragiola, R. A.; Carlson, R. W. *Icarus* **2006**, *180*, 265.
- (4) Gomis, O.; Leto, G.; Strazzulla, G. *Astron. Astrophys.* **2004**, *420*, 405.
- (5) Gomis, O.; Satorre, M. A.; Strazzulla, G.; Leto, G. *Planet. Space Sci.* **2004**, *52*, 371.
- (6) Moore, M. H.; Hudson, R. L. *Icarus* **2000**, *145*, 282.
- (7) Loeffler, M. J.; Baragiola, R. A. *Geophys. Res. Lett.* **2005**, *32*, 17202.
- (8) Cooper, P. D.; Johnson, R. E.; Quickenden, T. I. *Icarus* **2003**, *166*, 444.
- (9) Natta, G.; Rigamonti, R. *Gazz. Chim. Ital.* **1936**, *66*, 762.
- (10) Foley, W.; Giguere, P. A. *Can. J. Chem.* **1951**, *29*, 123.
- (11) Giguere, P. A.; K. B. Harvey. *J. Mol. Spectrosc.* **1959**, *3*, 36.
- (12) Pettersson, M.; Tuominen, S.; Rasanen, M. *J. Phys. Chem. A* **1997**, *101*, 1166.
- (13) Sack, N. J.; Baragiola, R. A. *Phys. Rev. B: Condens. Matter Mater. Phys.* **1993**, *48*, 9973.
- (14) Miller, R. L.; Horning, D. F. *J. Chem. Phys.* **1961**, *34*, 265.
- (15) Brown, D. E.; George, S. M.; Huang, C.; Wong, E. K. L.; Rider, K. B.; Smith, R. S.; Kay, B. D. *J. Phys. Chem.* **1996**, *100*, 4988.